# Improving the Efficiency of Closed-Chain Robotic Systems by the Trajectory Energy Index

# Improving the efficiency of closed-chain robotic systems by the Trajectory Energy Index

Paolo Boscariol, Lorenzo Scalera and Alessandro Gasparetto

**Abstract** This paper deals with the analysis of the impact of the task location within the robot workspace on its energy consumption. The work presents a performance index, which can be used to estimate the most favorable location of a given motion task, regardless of its complexity. The proposed performance index, called Trajectory Energy Index (TEI), is based on the inertial and kinematic properties of the robot, and its computation provides a guideline for defining the minimum-energy position of a task within the robot workspace. The effectiveness in prediction of the TEI is tested for a simple rest-to-rest motion and for a more complex task, which are executed by a two-degree-of-freedom planar robot with closed-loop kinematics.

## 1 Introduction

The manufacturing industry is currently responsible for a large percentage of the worldwide energy consumption [1]. Part of it is due to automatic machines and robots, whose diffusion is expected to further increase in near future; hence the need for engineering solutions capable of boosting the energy efficiency of such devices [2]. A transition to a greener mechatronics is not only cost-effective, but it is also fostered by the Sustainable Development Goals of the United Nations [3].

There are several ways to optimize the energy consumption of automatic machines or robots: the use of lightweight components [4], the adoption of regenerative motor drives [5], the inclusion of springs and reaction wheels into the mechanism [6, 7, 8], just to cite a few common options. Among such methods, many of them are of

Paolo Boscariol
DTG, Università degli Studi di Padova e-mail: paolo.boscariol@unipd.it

Lorenzo Scalera
DPIA, Università degli Studi di Udine, Italy e-mail: lorenzo.scalera@uniud.it

Alessandro Gasparetto
DPIA, Università degli Studi di Udine, Italy e-mail: alessandro.gasparetto@uniud.it

little use to most robot practitioners, who work almost exclusively with commercial products that cannot be hacked or modified to incorporate the required software of hardware solutions.

Given these limitations, the most feasible option for enhancing the energy performance related to the execution of a robotic task relies on the basics of programming the robot operation. Altering a planned trajectory, for example, is often the simplest way to improve the energy efficiency, as this kind of operation allows for up to 30% reduction of the total energy consumption. This possibility is investigated in a large amount of research works, which include, for instance, [9, 10, 11, 12].

Another option is to alter, rather than the whole motion profile, the location of the task within the robot workspace. Indeed, given the non-isotropic properties of a manipulator, it is rather evident that some areas of its workspace are to be preferred over some others to enhance a single property as the speed generation capability, the precision and accuracy, the rigidity and, among others, the energy efficiency as well. This basic intuition has led to the development of countless performance indexes and metrics that can provide some information on the behaviour of the manipulator and can be useful in the design of the robotic system itself [13, 14, 15].

As far as the development of a performance index that measures the energy efficiency of a robot, in this paper we refer to the Trajectory Energy Index (TEI), which has been introduced by the same authors in [16]. Such index has the advantage of relying on a limited set of parameters and has a rather simple formulation. Its capability of suggesting the optimal task location for a rest-to-rest motion has been previously showcased in the mentioned work by applying it to a SCARA robot with 3 degrees of freedom (DOF). In this paper, the applicability of the TEI is extended and slightly re-formulated, with respect to the previous work, for a clearer and simpler application to planar robots with closed-loop kinematic chain. Moreover, with respect to [16], not only rest-to rest, but also a more complex task, i.e., a three-leaf clover motion, is tested to evaluate the prediction capabilities of the TEI.

## 2 Formulation of the Trajectory Energy Index

In this section, the formulation of the performance index used to estimate the energy consumption of a robotic system that executes a motion task is briefly recalled. For a more detailed analysis of the development of the index, the reader can refer to [16]. Given a general mechanical or robotic system, its kinetic energy $\mathcal{K}$ can be written in terms of its mass matrix $\mathbf{M}$ and of its joint speed vector $\dot{\mathbf{q}}$ as:

$$\mathcal{K} = \frac{1}{2}\dot{\mathbf{q}}^T \mathbf{M}(\mathbf{q})\dot{\mathbf{q}} = \frac{1}{2}\dot{\mathbf{p}}^T \mathbf{J}^{-T}\mathbf{M}(\mathbf{q})\mathbf{J}^{-1}\dot{\mathbf{p}} \tag{1}$$

The second equality is found by expressing the kinetic energy in terms of the speed vector of the robot end-effector $\dot{\mathbf{p}}$, using the inverse differential kinematics $\dot{\mathbf{q}} = \mathbf{J}^{-1}\dot{\mathbf{p}}$.

Equation (1) reveals another form of the mass matrix, i.e., $\mathbf{G} = \mathbf{J}^{-T}\mathbf{M}(\mathbf{q})\mathbf{J}^{-1}$, which is a positive definite matrix. For ease of representation, let us refer to a planar

robot with just 2 DOFs. In this case, the kinetic energy of the robot can be expressed in terms of the two Cartesian components of the speed of the end-effector, $\dot{p}_x$ and $\dot{p}_y$. $\mathcal{K}$ can conveniently be represented as a quadratic surface, whose isoenergetic curves are actual inertia ellipsoids. Furthermore, for a given value of the kinetic energy $\bar{\mathcal{K}}$, the major and minor axes of the inertia ellipsoid are determined by the eigenvalues of the generalized mass matrix $\mathbf{G}$: the length of the major axis $a$ and of the minor axis $b$ are related to the eigenvalues $\lambda_1$ and $\lambda_2$ as: $a = 1/\sqrt{\lambda_1}$ and $b = 1/\sqrt{\lambda_2}$, and the directions of the axes are identified by the eigenvectors $\mathbf{v}_1$ and $\mathbf{v}_2$.

Let us now consider the two velocity vectors $\dot{\mathbf{p}}_A$ and $\dot{\mathbf{p}}_B$ represented in Fig. 1(a). Both vectors have the same module but different directions. The one associated with the minimum kinetic energy is $\dot{\mathbf{p}}_B$, which is aligned with the major axis of the ellipsoid. Hence, motions aligned with the major axis of the generalized inertia ellipsoid are more energy favourable. According to this intuition, a Local Energy

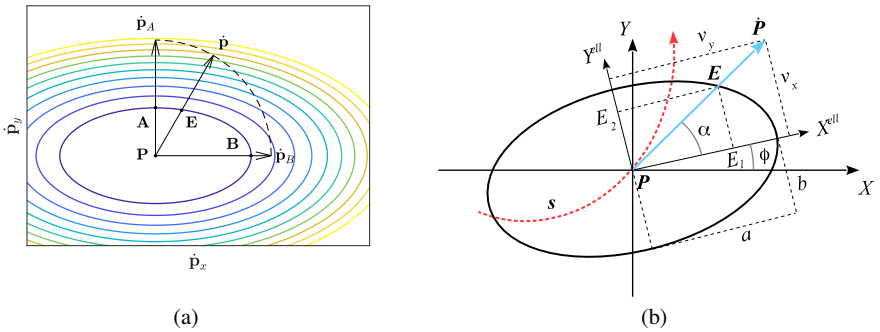


**Fig. 1** (a) Inertia ellipsoids and velocity vectors $\dot{\mathbf{p}}$, $\dot{\mathbf{p}}_A$ and $\dot{\mathbf{p}}_B$; (b) definition of points and vectors.

Index (LEI) can be defined as the inverse of the distance between the intersection point $\mathbf{E}$ and the center of the inertial ellipsoid, $\mathbf{P}$:

$$\mathrm{LEI}(\mathbf{q}, \dot{\mathbf{q}}) := \frac{1}{\|\mathbf{P} - \mathbf{E}\|_2} \tag{2}$$

The LEI is a local index that only refers to a punctual posture and to a single value of the end-effector speed. This metric can be further extended along a whole robot trajectory, allowing thus to capture the overall impact of the LEI along a task that is executed in the time frame $[t_0, t_f]$, through the Trajectory Energy Index (TEI):

$$\mathrm{TEI} := \frac{1}{t_f - t_0} \int_{t_0}^{t_f} \mathrm{LEI}(t)dt = \frac{1}{t_f - t_0} \int_{t_0}^{t_f} \frac{1}{\|\mathbf{P}(t) - \mathbf{E}(t)\|_2} dt \tag{3}$$

The method used to efficiently evaluate the actual values of the LEI and the TEI for a simple planar robot will be explained in detail in the next section.

## 3 Application to a closed-chain robotic system

The definition of the TEI is here applied to the 2-DOF planar robot with closed-loop kinematics shown in Fig. 2. The robot is placed in the horizontal plane and it is actuated by two motors located at points ***A*** and ***E***. The fixed location of the two actuators can boost the energy efficiency of this manipulator, but this can be further increased by a clever choice of the location of the task according to the prediction of the proposed index, as it is shown in the following. The first step for

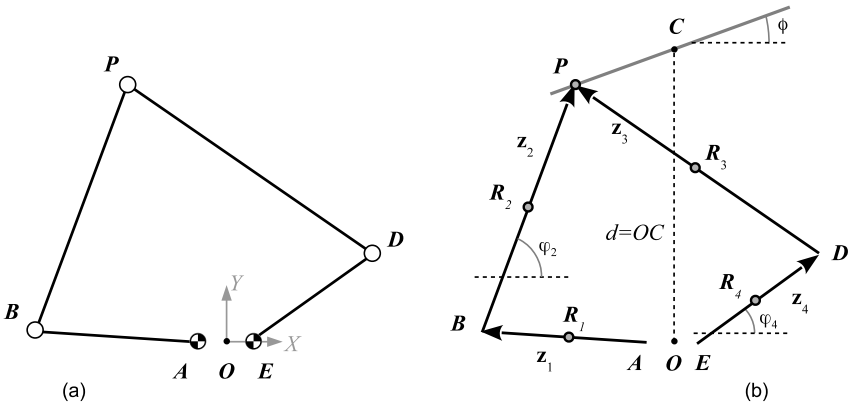


**Fig. 2** (a) 2-DOF planar robot with closed kinematic chain, (b) vectorial representation.

the computation of the LEI is the definition of the generalized inertia matrix: in this case the generalized coordinates are assumed to be $[q_1, q_2]^T = [\varphi_1, \varphi_4]^T$, i.e., the angular position of the two cranks. Each link of the manipulator is described by a vector $\mathbf{z}_i$ with length $z_i$ and angular position $\varphi_i$, as shown in Fig. 2. The mass distribution of the links is assumed to be homogeneous, and an additional point mass $m_P$ is located at the end-effector (point **P**) to represent the mass of a tool. The generalized mass matrix can be built by including the contribution of each moving body belonging to the manipulator, as follows:

$$\mathbf{G} = \mathbf{G}_P + \sum_{i=1}^{4} \mathbf{G}_i \tag{4}$$

which collects the contributions due to the end-point mass $m_P$ and of each i-*th* link. The speed vector $\dot{\mathbf{R}}_i$ of the center of mass of each link (with coordinates $x_i, y_i, \varphi_i$) of the mechanism can be written using the Jacobian $\mathbf{J}_{\mathbf{R}_i,\mathbf{q}}$ with respect to the speed of the generalized coordinates $\dot{\mathbf{q}}$. Alternatively, $\dot{\mathbf{R}}_i$ can be expressed in terms of the end-effector speed $\dot{\mathbf{P}}$, as follows:

$$\dot{\mathbf{R}}_i = \begin{bmatrix} \dot{x}_i \\ \dot{y}_i \\ \dot{\varphi}_i \end{bmatrix} = \mathbf{J}_{\mathbf{R}_i,\mathbf{q}}\dot{\mathbf{q}} = \mathbf{J}_{\mathbf{R}_i,\mathbf{q}}\mathbf{J}_{\mathbf{q},\mathbf{P}}\dot{\mathbf{P}} = \mathbf{J}_{\mathbf{R}_i,\mathbf{P}}\dot{\mathbf{P}} \tag{5}$$

where $\mathbf{J}_{\mathbf{q},\mathbf{P}}$ and $\mathbf{J}_{\mathbf{R}_i,\mathbf{P}}$ are the Jacobian matrices that relate the generalized coordinates and the end-effector coordinates, and the generic center of mass of the i-*th* link and the generalized coordinates, respectively. For example, the speed of link 2 can be computed as:

$$\dot{\mathbf{R}}_2 = \begin{bmatrix} -z_1 s\varphi_1 - \frac{z_2}{2} s\varphi_2 k_{\varphi_2,q_1} & -z_2 s\varphi_2 k_{\varphi_2,q_2} \\ z_1 c\varphi_1 + \frac{z_2}{2} c\varphi_2 k_{\varphi_2,q_1} & z_2 c\varphi_2 k_{\varphi_2,q_2} \\ k_{\varphi_2,q_1} & k_{\varphi_2,q_2} \end{bmatrix} \begin{bmatrix} -z_1 s\varphi_1 & -z_2 s\varphi_2 \\ z_1 c\varphi_1 & z_2 c\varphi_2 \end{bmatrix}^{-1} \dot{\mathbf{P}} = \mathbf{J}_{\mathbf{R}_2,\mathbf{P}}\dot{\mathbf{P}} \tag{6}$$

where the terms $k_{\varphi_i,q_j}$ are the coefficients of the linear combination of speed $\dot{\varphi}_i$ in terms of joint speeds $\dot{q}_j$. $\mathbf{J}_{\mathbf{R}_2,\mathbf{P}}$ represents the Jacobian matrix that relates the speed of the center of mass of link 2 to the the end-effector speed. Hence, the contribution $\mathbf{G}_2$ to the generalized mass matrix $\mathbf{G}$ is given by:

$$\mathbf{G}_2 = \mathbf{J}^T_{\mathbf{R}_2,\mathbf{P}} \begin{bmatrix} m_2 & 0 & 0 \\ 0 & m_2 & 0 \\ 0 & 0 & I_2 \end{bmatrix} \mathbf{J}_{\mathbf{R}_2,\mathbf{P}} \tag{7}$$

where $m_2$ is the mass of link 2, and $I_2$ its mass moment of inertia. The contribution of the end-point mass $m_P$ to $\mathbf{G}$ is simply:

$$\mathbf{G}_P = \begin{bmatrix} m_P & 0 \\ 0 & m_P \end{bmatrix} \tag{8}$$

Once the generalized mass matrix $\mathbf{G}$ is computed, the inertia ellipsoid can be represented as in Fig. 1(b). Two reference frames are shown: $\{X, Y\}$ is centered in $\mathbf{P}$ and aligned with the global reference frame, while $\{X^{ell}, Y^{ell}\}$ is instead aligned with the major axis of the ellipsoid; hence the latter is rotated by $\phi$. The end-effector speed vector $\dot{\mathbf{P}}$ is also shown in the same figure. It has components $[v_x, v_y]^T$ when measured in the rotated reference frame. The computation of the LEI requires the determination of the length of the vector $\mathbf{P} - \mathbf{E}$, which has components $E_1$ and $E_2$. The latter can be computed as an intersection with the ellipsoid as:

$$E_1 = \frac{ab}{\sqrt{a^2 v_y^2 + b^2 v_x^2}} v_x; \qquad E_2 = \frac{ab}{\sqrt{a^2 v_y^2 + b^2 v_x^2}} v_y; \tag{9}$$

Finally, the norm of vector $\boldsymbol{P} - \boldsymbol{E}$, i.e., $1/LEI$, can be computed as:

$$\|\mathbf{P} - \mathbf{E}\|_2 = \frac{1}{LEI} = \frac{ab\sqrt{v_x^2 + v_y^2}}{\sqrt{a^2 v_y^2 + b^2 v_x^2}} \tag{10}$$

Extending the evaluation of Eq. (10) to a whole trajectory and then integrating it over time, as shown in Eq. (3), provides the means to estimate the effects of locating a motion task within the robot workspace. This will be shown in Sect. 4.

To compare the predictions of the TEI with the energy consumption of the robot, a dynamic and an electromechanical model of the system are derived. The joint torques $\boldsymbol{\tau}$ can be computed as:

$$\boldsymbol{\tau} = \mathbf{M}(\mathbf{q})\ddot{\mathbf{q}} + \mathbf{C}(\mathbf{q}, \dot{\mathbf{q}})\dot{\mathbf{q}} + f_v\dot{\mathbf{q}} + f_c \text{sign}(\dot{\mathbf{q}}) \tag{11}$$

where $\mathbf{M}$ is the mass matrix, $\mathbf{C}(\mathbf{q}, \dot{\mathbf{q}})\dot{\mathbf{q}}$ accounts for Coriolis and centrifugal terms, whereas $f_v\dot{\mathbf{q}}$ and $f_c \text{sign}(\dot{\mathbf{q}})$ include the viscous and Coulomb friction coefficients.

The electromechanical model of the actuators is derived assuming brushless DC motors, and the overall energy consumption $E$ of the robot can be computed as:

$$E = \sum_{j=1}^{2} \int_{t_0}^{t_f} W_{e,j} dt = \sum_{j=1}^{2} \int_{t_0}^{t_f} v_j(t)\, i_j(t) dt \tag{12}$$

$W_{e,j}$ indicates the electric power for the j-*th* motor, $v_j(t) = R\, i_j(t) + k_e\, \dot{q}_{m,j}$ is the voltage drop across the j-*th* motor (where $R$ is the resistance of the motor windings, $k_e$ the back-emf constant, whereas $\dot{q}_{m,j} = \dot{q}_j\, k_r$ indicates the velocity of the j-*th* motor shaft computed with the reduction ratio $K_r$), $i_j(t) = \tau_{m,j}(t)/k_t$ is the current drawn by the j-*th* motor, assuming $k_t$ as motor torque constant and $\tau_{m,j} = \tau_j/k_r$. Finally, $\eta_d$ represents the efficiency of the driver, $J_m$ and $J_r$ are the moments of inertia of the motor and of the gearbox, respectively.

## 4 Simulation results

In this section, the simulation results and the comparison between the results obtained with the TEI, and those obtained with the electro-dynamic model of the robotic system are illustrated. The geometrical and dynamical parameters used in the numerical simulations are reported in Tab. 1. Two test cases are considered: a rest-to-rest motion and a more complex task, i.e., the motion along a path defined as a three leaf clover.

**Table 1** Geometrical and dynamical parameters used in the numerical simulations.

| | | |
|---|---|---|
| $z_1 = z_4 = 0.502\ m$ | $m_1 = m_4 = 1.626\ kg$ | $I_1 = I_4 = 0.0342\ kgm^2$ |
| $z_2 = z_3 = 1\ m$ | $m_2 = m_3 = 1.080\ kg$ | $I_2 = I_3 = 0.09\ kgm^2$ |
| $AE = 0.175\ m$ | $m_P = 0.2\ kg$ | $\eta_r = 0.95$ |
| $k_r = 1/24$ | $J_m = 6.2407 \cdot 10^{-5}\ kgm^2$ | $J_r = 8.4855 \cdot 10^{-4}\ kgm^2$ |
| $k_e = 0.0564\ Vs/rad$ | $k_t = 0.0915\ Nm/A$ | $R = 10.05\ \Omega$ |
| $f_v = 7.3458 \cdot 10^{-6}$ | $f_c = 6.54 \cdot 10^{-4}\ Nm$ | |

### 4.1 Rest-to-rest motion

The first comparison is set by analyzing the performance of the manipulator when executing a simple rest-to-rest motion planned in the operational space. The end-effector of the robot is moved in just 500 $ms$ on a straight line with length 0.3 $m$. The location of the task is defined by the distance between the base of the robot and the mid-point of the straight line: such parameter is defined as $d$ in the following. It is also assumed that the direction of the line can be altered and it is represented by the angle $\phi$, as shown in figure 2(b). Hence when $\phi = 0$ the point $P$ is moved left to right (according to Fig. 2), whereas $P$ is moved toward the robot base whenever $\phi = \pi/2\, rad$. The motion is planned according to a symmetric trapezoidal speed profile with acceleration time equal to $t_a = 125\ ms$. This simple parametrization allows for a straightforward representation of the actual energy consumption, evaluated according to the model presented in Sect. 3, and of the TEI, vs. $d$ and $\phi$, as shown in Fig. 3(a) and 3(b), respectively.

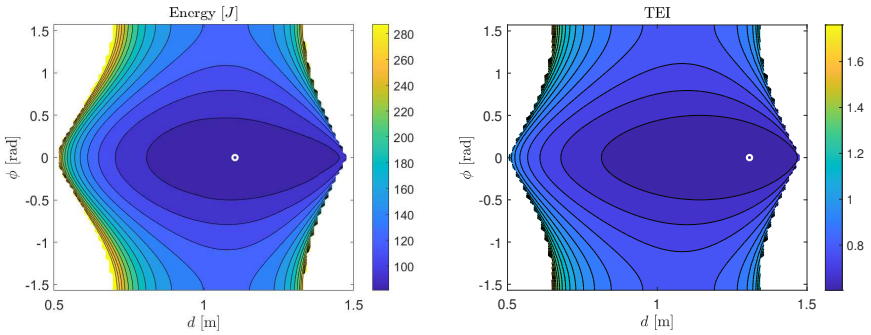


**Fig. 3** Rest-to-rest motion: (a) energy map obtained with the electro-dynamic model of the robot; (b) TEI map. The white circles indicate the minimum-energy location.

The white circles highlight the minimum location in both graphs: the energy minimum is found for $\phi = 0$ and $d = 1.104\ m$, while the TEI minimum happens for $\phi = 0$ and $d = 1.308\ m$. Still, a good agreement between the two metrics is found, showing that the computation of the TEI provides an useful guideline that can replace the full energetic analysis. As a general rule, the straight line motion should be executed whenever possible along a line parallel to the X-axis and far away from the base of the robot, as suggested by both metrics. Motions in the radial direction or parallel to the Y-axis are, instead, sensibly less energy efficient.

### 4.2 Three-leaf clover motion

The second test case involves the execution of a more complex task: the motion of the end-effector along a path shaped as a three-leaf clover, shown in Fig. 4(a). A continuous motion is assumed, with end-effector Cartesian speed and accelerations shown in the same graph. The task is in this case parametrized by just the distance between the center of the clover and the base of the robot, indicated as $d$. The estimated energy consumption and the measured TEI are plotted, against $d$, in Fig. 4(b), showing, again, a good agreement between the two metrics.

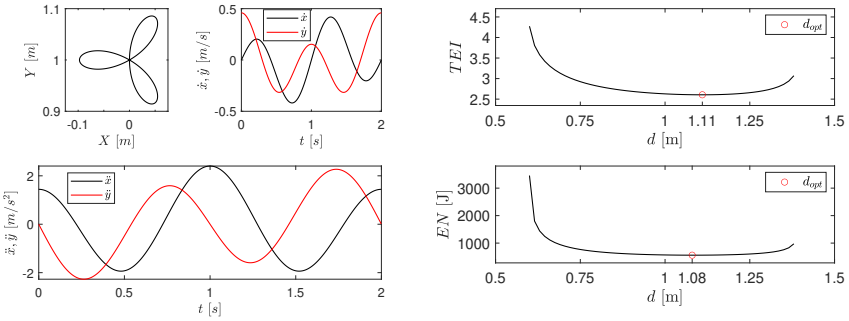


(a) (b)

**Fig. 4** Three-leaf clover motion: (a) end-effector path, speed and acceleration; (b) comparison between TEI and actual energy consumption vs. the distance $d$ from the robot base along the Y-axis.

The minimization of the TEI happens at $d = 1.11\ m$, while the energy minimum is detected for $d = 1.08\ m$ by using the full energy model. In this case the minimization of the TEI provides a solution which almost perfectly matches the prediction of a more sophisticated and complex model.

## 5 Conclusion

This paper has proposed the use of the Trajectory Energy Index for the reduction of the energy consumption of manipulators executing complex motion tasks. The proposed index, which is based just on the kinematic and inertial properties of the manipulator, can be successfully used to define a motion task that reduces the energy consumption of the robot. The suggested procedure avoids the definition and the use of a full electro-dynamic model of the manipulator under investigation. The method is applied to two numerical test-cases that involve a 2-DOF planar parallel robot, showing the overall good capability of the suggested index of predicting the impact of the task parameters on the overall energy consumption.

## References


1. Murat Kucukvar, Bunyamin Cansev, Gokhan Egilmez, Nuri C Onat, and Hamidreza Samadi. Energy-climate-manufacturing nexus: New insights from the regional and global supply chains of manufacturing industries. *Applied energy*, 184:889–904, 2016.
2. Giovanni Carabin, Erich Wehrle, and Renato Vidoni. A review on energy-saving optimization methods for robotic and automatic systems. *Robotics*, 6(4):39, 2017.
3. Giuseppe Quaglia, Alessandro Gasparetto, Victor Petuya, and Giuseppe Carbone, editors. *1st Workshop IFToMM for Sust. Dev. Goals, I4SDG*. Springer Science, 2022.
4. Haibin Yin, Jing Liu, and Feng Yang. Hybrid structure design of lightweight robotic arms based on carbon fiber reinforced plastic and aluminum alloy. *IEEE Access*, 7:64932, 2019.
5. Poya Khalaf and Hanz Richter. Parametric optimization of stored energy in robots with regenerative drive systems. In *Int. Conf. on Adv. Intel. Mech.*, pages 1424–1429. IEEE, 2016.
6. Makoto Iwamura and Werner Schiehlen. Control and experiments with energy-saving scara robots. In *Symp. on Robot Design, Dynamics and Control*, pages 153–161. Springer, 2016.
7. Dario Richiedei and Alberto Trevisani. Optimization of the energy consumption through spring balancing of servo-actuated mechanisms. *Journal of Mechanical Design*, 142(1), 2020.
8. Lorenzo Scalera, Giovanni Carabin, Renato Vidoni, and Theeraphong Wongratanaphisan. Energy efficiency in a 4-DOF parallel robot featuring compliant elements. *International Journal of Mechanics and Control*, 20(2), 2019.
9. Paolo Boscariol and Dario Richiedei. Energy-efficient design of multipoint trajectories for cartesian robots. *The Int. J. of Adv. Manuf. Tech.*, 102(5-8):1853–1870, 2019.
10. Giovanni Carabin and Lorenzo Scalera. On the trajectory planning for energy efficiency in industrial robotic systems. *Robotics*, 9(4):89, 2020.
11. Phat Minh Ho, Naoki Uchiyama, Shigenori Sano, Yuta Honda, Atsushi Kato, and Takahiro Yonezawa. Simple motion trajectory generation for energy saving of industrial machines. *SICE J. of Contr., Meas., Syst. Int.*, 7(1):29–34, 2014.
12. Koen Paes, Wim Dewulf, Karel Vander Elst, Karel Kellens, and Peter Slaets. Energy efficient trajectories for an industrial ABB robot. *Proc. Cirp*, 15:105–110, 2014.
13. Giovanni Boschetti. A novel kinematic directional index for industrial serial manipulators. *Applied Sciences*, 10(17):5953, 2020.
14. Sarosh Patel and Tarek Sobh. Manipulator performance measures-a comprehensive literature survey. *Journ. of Int. & Rob. Systems*, 77(3-4):547–570, 2015.
15. Edoardo Idà and Marco Carricato. A new performance index for underactuated cable-driven parallel robots. In *Int. Conf. on Cable-Driven Parallel Robots*, pages 24–36. Springer, 2021.
16. Fabrizio Vidussi, Paolo Boscariol, Lorenzo Scalera, and Alessandro Gasparetto. Local and trajectory-based indexes for task-related energetic performance optimization of robotic manipulators. *Journal of Mechanisms and Robotics*, 13(2), 2021.